Evidence for functional GABAA but not GABAC receptors on mouse cone photoreceptors

Sercan Deniz, Eric Wersinger, Serge Picaud, Michel Roux

Evidence for functional $GABA_A$ but not $GABA_C$ receptors on mouse cone photoreceptors

Sercan DENIZ[1-4a], Eric WERSINGER[1-4b], Serge PICAUD[5], Michel J. ROUX[1-4§]

1) Institut de Génétique et de Biologie Moléculaire et Cellulaire, Illkirch, France

2) Centre National de la Recherche Scientifique, UMR7104, Illkirch, France

3) Institut National de la Santé et de la Recherche Médicale, U1258, Illkirch, France

4) Université de Strasbourg, Illkirch, France

5) Sorbonne Université, INSERM, CNRS, Institut de la Vision, 17 rue Moreau, F-75012 Paris, France

[§] To whom correspondence should be addressed. Email: mjroux@igbmc.fr

[a] Present address: Department of Ophthalmology, Feinberg School of Medicine, Northwestern University, Chicago IL 60611, USA

[b] Present address: Facultés de Médecine et de Pharmacie, UMR INSERM/UCA 1107-Neuro-Dol, 28 place Henri Dunant - B.P. 38,63001 Clermont-Ferrand Cedex 1, France

Running title: GABA receptors in mouse cones

Pages: 25

Tables: 0

Figures: 4

Title: Evidence for functional $GABA_A$ but not $GABA_C$ receptors on mouse cone photoreceptors

Abstract:

At the first retinal synapse, horizontal cells contact both photoreceptor terminals and bipolar cell dendrites, modulating information transfer between these two cell types to enhance spatial contrast and mediate color opponency. The synaptic mechanisms through which these modulations occur are still debated. The initial hypothesis of a GABAergic feedback from horizontal cells to cones has been challenged by pharmacological inconsistencies. Surround antagonism has been demonstrated to occur via a modulation of cone calcium channels through ephaptic signaling and pH changes in the synaptic cleft. GABAergic transmission between horizontal cells and cones has been reported in some lower vertebrates like the turtle and tiger salamander. In these reports, GABA is released from horizontal cells through reverse transport and target GABA receptors are located on cone terminals. In mammalian retinas, there is growing evidence that horizontal cells can release GABA through conventional vesicular transmission, acting both on autaptic GABA receptors and on receptors expressed at the dendritic tips of bipolar cells. The presence of GABA receptors on mammalian cone terminals remains equivocal. Here, we looked specifically for functional GABA receptors on mouse photoreceptors by recording in the whole-cell or amphotericin/gramicidin perforated patch-clamp configurations. Cones could be differentiated from rods through morphological criteria. Local GABA applications evoked a Cl^- current in cones but not in rods. It was blocked by the $GABA_A$ receptor antagonist bicuculline methiodide and unaffected by the $GABA_C$ receptor antagonist TPMPA. The voltage dependency of the current amplitude was as expected from a direct action of GABA on cone pedicles, but not from an indirect modulation of cone currents following the activation of the GABA receptors of horizontal cells. This supports a direct role of GABA release from horizontal cells in the control of cone activity in the mouse retina.

Keywords: GABA, feedback, cone photoreceptor, horizontal cell

INTRODUCTION

Our ability to detect edges in the visual world is enhanced through a process called lateral inhibition, mediated by horizontal cells (HCs) which exert both a negative (Baylor *et al.*, 1971) and a positive (Jackman *et al.*, 2011) feedback onto cone photoreceptors. The underlying synaptic mechanisms are still not fully understood. Inconsistencies in the pharmacology and ions underlying the negative feedback current have challenged the initial hypothesis of a GABAergic transmission between HCs and cones (reviewed in Piccolino, 1995; Thoreson & Mangel, 2012). A modulation of cone calcium channels (Verweij *et al.*, 1996, 2003), by either hemichannel-mediated ephaptic communication (Kamermans *et al.*, 2001; Pottek *et al.*, 2003; Fahrenfort *et al.*, 2009; Klaassen *et al.*, 2011; Kemmler *et al.*, 2014) or through pH changes in the synaptic cleft (Hirasawa & Kaneko, 2003; Davenport *et al.*, 2008; Wang *et al.*, 2014) has arisen as the main mechanism for the negative feedback. Far from being mutually exclusive, both ephaptic and pH modulations are likely to shape cone calcium signals (Kemmler *et al.*, 2014).

Many of the molecular and physiological underpinnings required for a GABAergic transmission from HCs to cones are however present in various species. On the presynaptic side, in lower vertebrates, GABA can be released in a Ca^{2+}-independent manner via membrane transporters (Schwartz, 1987). In the mammalian outer retina, the vesicular transporter VGAT/VIAAT was localized in HC tips in mouse, guinea pig, human and macaque retinas (Haverkamp *et al.*, 2000; Cueva *et al.*, 2002; Jellali *et al.*, 2002; Guo *et al.*, 2010); HCs were reported to express the synaptic proteins required for vesicular release in rabbit and guinea pig (Hirano *et al.*, 2005; Lee & Brecha, 2010). Though HCs were previously reported not to contain GABA in rodents (Agardh *et al.*, 1986; Versaux-Botteri *et al.*, 1989; Fletcher & Kalloniatis, 1997), we have demonstrated that this was due to GABA loss during tissue preparation, that could be compensated by supplementing the medium with a GABA precursor, such as glutamine or glutamate, and with pyridoxal phosphate, a cofactor of the glutamate acid decarboxylases (Deniz *et al.*, 2011). Preventing GABA release from HCs by targeted

deletion of VGAT removed the feedback to cone photoreceptors (Hirano *et al.*, 2016), possibly through an autaptic action of GABA on HCs, changing the membrane permeability to HCO_3^- and hence affecting the pH in the synaptic cleft (Liu *et al.*, 2013). If GABA receptors are expressed in cone terminals, they could modulate cone output both by influencing directly the membrane potential and by affecting the pH in the synaptic cleft, as those expressed on HCs.

On the postsynaptic side, while the presence of GABA receptors on cone terminals has been reported in many lower vertebrates (reviewed in Wu, 1992), it remains controversial regarding mammalian cones. *In situ* hybridization in rat showed signal in the ONL for β_1 but not for several other subunits of $GABA_A$ receptors (α_{1-4}, β_{2-3}, γ_2 et δ) (Greferath *et al.*, 1993, 1995). β_1 and β_2 mRNA were detected in the rat ONL by PCR (Grigorenko & Yeh, 1994). I*n situ* hybridization for the $GABA_A$ α_1 subunit was also negative in the rabbit retina (Brecha *et al.*, 1991). α and β subunits were detected in cone pedicles but not in rod spherules by immunohistochemistry in the cat (Vardi *et al.*, 1992). Further electron microscopy studies in macaque and rabbit retinas suggested that the GABA receptor subunit staining in the OPL might be attributed solely to the strongly labelled bipolar cell dendritic tips (Vardi & Sterling, 1994; Greferath *et al.*, 1994). α_1 and ρ subunits were not detected in mouse cones by immuno electron microscopy (Kemmler *et al.*, 2014). A GABA-evoked current was detected in only a fraction of cones in macaque flatmount retina, without pharmacological characterization (Verweij *et al.*, 2003); both $GABA_A$ and $GABA_C$ receptors were reported by combining electrophysiology and immunohistochemistry in porcine cones in culture (Picaud *et al.*, 1998) and in putative mouse cones from flatmount *rd1* retinas or dissociated from WT C57BL/6J retinas (Pattnaik *et al.*, 2000). These apparent discrepancies may be due to variations between species, a difficult path for GABA to reach the cone terminals in WT flatmounts, low levels of expression of GABA receptor subunits in mammalian cones, difficulty in identifying dissociated cones, and/or changes in expression during retinal degeneration or in culture. To circumvent those issues, we have assessed directly the presence of GABA receptors in photoreceptors on acute slices of adult mouse retinas, using either whole-cell or perforated patch clamp recordings.

MATERIAL AND METHODS

Retinal slice preparation

Procedures involving animals and their care were conducted in agreement with the ARVO Statement for the Use of Animals in Ophthalmic and Vision Research, the French Ministry of Agriculture and the European Community Council Directive no. 86/609/EEC, OJL 358. Mice strains used in this study were either C57BL/6J or Balb/c ByJ bred at the Mouse Clinical Institute animal house (Illkirch, France). As results from both strains were similar, results were pooled together. Mice were maintained on a 12h/12h light-dark cycle, with light ON from 7 AM to 7 PM. Light-adapted, adult (9-19 weeks) mice were killed by cervical dislocation in the morning (9-10 AM). The eyes were enucleated and immediately put in ice-cold bicarbonate-buffered saline (BBS), composed of (in mM): NaCl 126, KCl 2.5, $CaCl_2$ 2.4, $MgCl_2$ 1.2, NaH_2PO_4 1.2, $NaHCO_3$ 18, glucose 11 previously bubbled with 95% O_2 / 5% CO_2. The cornea, lens and vitreous were removed. The retina was detached from the pigmented epithelium and embedded in agarose 1.5% prepared in PBS (0.1 M; pH 7.4) kept at 42°C. After agarose solidification on ice, the retina was cut in 150 or 200 µm thick slices using a Leica VT1000S vibratome (Leica, Wetzlar, Germany). The slices were kept at room temperature in bubbled BBS for at least half an hour before recording, in normal lighting conditions.

Patch-clamp recordings

Slices were observed under infrared differential interference contrast (DIC) using a 63x objective and a C8484 camera (Hamamatsu, Massy, France) on a Leica DMLFS microscope (Leica, Wetzlar, Germany). The preparation was continuously perfused at ~2 ml / minute with bubbled BBS. Pipettes (6-8 MΩ) were pulled from GC150TF borosilicate glass capillaries (Harvard Apparatus, Les Ulis, France) on a horizontal puller (DMZ Universal Puller, Zeitz Instrumente, Munich, Germany). Two different intracellular solutions were used: one containing (in mM) KCl 42, K gluconate 98, EGTA-Na_4 10, $MgCl_2$ 1, HEPES 5, ATP-Na_2 5 (E_{Cl} = -28.9 mV, junction potential of 12.4 mV, referred to in the text as E_{Cl} = -29 mV) or KCl 138, EGTA-Na_4 10, $MgCl_2$ 3, $CaCl_2$ 1, HEPES 10, ATP-Na_2 3, GTP-Na_3 0.5 (E_{Cl} =

1.9 mV, junction potential of 3.9 mV, referred to in the text as E_{Cl} = 2 mV). For perforated patch recordings, amphotericin B (80-180 µg/ml) or gramicidin (80-100 µg/ml) was added to the pipette solution from a 120 mg/ml stock solution in DMSO. All solutions contained 10 µM of Alexa Fluor® (488 or 594) hydrazide (Molecular Probes, Eugene, OR), and pH was adjusted to 7.4 with NaOH. The extracellular solution was the BBS described above, continuously bubbled with 95% O_2 / 5% CO_2. Potentials were corrected post-recording for the calculated junction potential. For simplicity, potentials indicated in the text are rounded to integer values. All experiments were performed at room temperature (20-25°C), between 11 AM and 8 PM for the successful cone recordings, with no evident circadian variation (Supplementary Figure 4). Data were acquired using a Multiclamp 700A amplifier, a Digidata 1322A interface and the pClamp9 software (Molecular Devices, Sunnyvale, CA). Data were filtered prior to digitization at a frequency of 1/2 or 1/5th of the acquisition frequency, which was 200 Hz for puffed GABA (γ-aminobutyric acid) and 10 kHz for depolarizing pulse experiments. Agonists were applied locally with a puffer pipette connected to a Picospritzer III (Parker Hannifin, Fairfield, NJ) and antagonists were applied via bath application. TPMPA ((1,2,5,6-Tetrahydropyridin-4-yl)methylphosphinic acid) was obtained from Tocris (Ellisville, MI), all others chemicals were obtained from Sigma-Aldrich (Lyon, France). All values are indicated as mean ± S.E.M.

RESULTS

Targeting cone photoreceptors on mouse retinal slices

To determine if mouse photoreceptors express functional GABA receptors, we recorded from cones and rods in the whole-cell patch-clamp configuration, on acute slices from mouse retinas. Cones, which represent only 3% of the photoreceptor population in mice (Jeon *et al.*, 1998), have slightly larger and more oval cell bodies than rods. This morphological difference allowed for a partially targeted rather than "blind" cone recording. Although most of the cone cell bodies were located close to the outer limiting membrane (Fig. 1A), some of them were also found close to the OPL (Fig. 1B). As an Alexa dye was included in the pipette solution, cone identity could be confirmed at the end of the recording by visualizing the synaptic terminal, as previously reported by Cangiano *et al.*(2012). Cone pedicles (Fig. 1A-C, supplementary figure 1) are much larger than the small rounded terminals of rods (Fig. 1D-E, supplementary figure 2). The long outer segment of rods (Fig. 1D-E, supplementary figure 3) was also more readily observed than the shorter one from cones. While the formation of a gigaseal could be readily obtained with both types of photoreceptors, most of the cells were lost when attempting to go into the whole-cell configuration, possibly due to the fact that the nucleus occupies most of the cell soma volume. Some rods were recorded after contacting them at the level of the inner segment (Fig. 1D), which allowed for an easier transition to whole-cell mode. Some recordings were obtained using amphotericin B perforated-patch, which allowed for a higher success rate than whole-cell patch. Cone identity could be confirmed by dye diffusion after membrane rupture at the end of the recording.

To compare the responses to GABA applications in cones with and without terminals, we needed a criterion to distinguish the latter from terminal-lacking rods. To this end, we compared the current-voltage (I-V) relationships obtained from photoreceptors. We have more specifically focused on I-V curves recorded with the E_{Cl} = -29 mV pipette solution during 100 ms voltage steps, conditions for which we had the most cells in the different categories. For well-identified, terminal-bearing

photoreceptors, currents evoked by voltage steps above -50 mV were larger in cones than in rods (Fig. 2A-D), as were the following tail currents (Fig. 2A-C, E) (13 rods and 11 cones in D and E), requiring in some cones over a second to fully de-activate after a 100 ms depolarizing step (Fig. 2C). These currents were similar to the chloride currents described in cones from the larval tiger salamander (Barnes & Bui, 1991) and the ground squirrel (Szmajda & DeVries, 2011). The depolarization-evoked current was maximal at +26 mV (Fig. 2D), while the tail current peaked when returning from a step to +6 mV (Fig. 2E). The individual values of these currents are represented in Figure 2 F-G, distinguishing five groups of cells. Cones (n = 11) and rods (n = 13) that could be identified through the morphology of their synaptic terminal are represented with green and grey symbols, respectively. Rods identified as such through the presence of a typical outer segment but with no visible synaptic terminal are represented with orange symbols (n = 11). The remaining cells were tagged either as putative cones (red symbols, n = 8) or putative rods (cyan symbols, n = 5) depending on the shape of their soma as observed prior to recording – oval for cones (see stars in Fig.1B), rounded for rods. The presence of a short outer segment was not used to tag cones, as such a segment could correspond to a damaged/collapsed rod outer segment. For both types of currents, the range of amplitudes were comparable between identified and putative cones, and between identified and putative rods (Fig. 2F). However, there was some overlap between the cone and rod populations, thus neither the plateau nor tail current amplitude alone could be used to unambiguously identify as cones some of the terminal-less cells. When considering both currents together, there was very little overlap between the cone and rod populations, all identified and putative rods being included in the range [I_{tail} < 100 pA, $I_{plateau}$ < 350 pA], while all but one of the identified and putative cones were outside this range (Fig. 2G).

Cones response to GABA applications

GABA (1 mM) was puffed nearby the synaptic terminal of the recorded photoreceptors (5 to 250 ms duration). A GABA-evoked current was detected in 34 out of 35 cones with pedicles. The

amplitude of the current evoked by a 100 ms puff of 1 mM GABA on 14 pedicle-bearing cones recorded with the E_{Cl} = 2 mV intracellular solution ranged between -12.5 and -166 pA at -64 mV (-51.4 ± 46.5 pA, n = 14) (Fig. 3A; left). As GABA was applied onto the surface of the slice, the current amplitude was at least in part dependent upon the depth of the pedicle in the slice. Notably, a cone with an intact morphology but with a pedicle deeper than 30 µm (estimated from the epifluorescence focus) did not respond to GABA when puffed on the slice surface, but responded when the puff pipette was dipped into the slice. As the response kinetics were similar to those of other cones after GABA puffs on the slice surface, it was most probably a true response to GABA rather than a mechanical artifact. No GABA-evoked current was detected from cells tentatively identified as pedicle-less cones through the current amplitude criteria presented in Figure 2G (n = 4), in line with a GABA receptor localization restricted to the synaptic terminal, as in turtle retina (Tachibana & Kaneko, 1984). No current was evoked in rods either (Fig. 3A, right), whether they had their spherule (n = 7) or not (n = 8). This was an additional control against a possible mechanical puff-induced response. Bicuculline methiodide (100 µM) blocked 87.5 ± 3.2 % (n = 11) of the GABA evoked current (Fig. 3B, left). For cells in which bicuculline methiodide did not fully block the response to GABA, the presence of the antagonist did not change the kinetics of the GABA-evoked current, as can be seen in Figure 3C, which presents both the raw traces (left) and currents normalized to their peak (right). This suggests that the remaining current corresponds to an incomplete blockade, rather than to a kinetically slower $GABA_C$ component. Consistent with this hypothesis, the $GABA_C$ antagonist TPMPA (50 µM) had little effect (Fig. 3B, right) on the GABA-induced current with a mean blockade of 4.7 ± 4.7 % (n = 3). We could not systematically apply both inhibitors, as most of the cone recordings were short-lived. As expected for currents mediated by ionotropic GABA receptors, the GABA-evoked current reversed at a potential close to the Cl^- equilibrium potential (E_{Cl}): when E_{Cl} was set at -29 mV, the current reversed at -30.3 ± 4.1 mV (n = 5, Fig. 3D). When E_{Cl} was set at 2 mV, the current reversed at 0.7 ± 1.7 mV (n = 7, Fig. 3E).

E_{Cl} in mouse cones

The physiological role of the GABA-evoked current depends on its reversal potential. To assess this parameter, we used gramicidin perforated-patch recordings. The success rate of such recordings on cones was very low. In 4 cells with adequate intracellular access, GABA evoked very small currents (-3.4 ± 1.7 pA at -94 mV, -1.5 ± 0.8 pA at -64 mV). It is probable than these cells were cones rather than rods, as in whole-cell, we did not record any GABA response from identified rods (0/7) in opposition to cones (34/35), as mentioned above. The GABA-evoked current changed linearly with the membrane potential, reversing at -36.9 ± 6.3 mV (n = 4, Fig. 3F). .

DISCUSSION

There is contradictory evidence for the presence of functional $GABA_A$ receptors on cone synaptic terminals, depending on species. $GABA_A$ receptor-mediated currents were reported in many lower vertebrates, including in the turtle (Kaneko & Tachibana, 1986) and the salamander (Wu, 1986). Atypical ionotropic GABA receptors as well as $GABA_B$ receptors were detected in the bullfrog retina (Liu *et al.*, 2005, 2006). There are however very few published electrophysiological recordings from mammalian cones. Small GABA responses were detected in only a fraction of macaque cones on flatmount retinas (5/12), with a polarity matching the one expected for a Cl^- current in 4 out of the 5 responding cones (Verweij *et al.*, 2003). No pharmacology was performed to determine if those responses could be due to the activation of GABA receptors. Large $GABA_A$ and $GABA_C$ currents were recorded both in primary culture of pig cones (Picaud *et al.*, 1998), and on putative mouse cones, either on flatmount *rd1* mouse retinas or dissociated from C57BL/6J retinas (Pattnaik *et al.*, 2000).

We report here for the first time, in morphologically identified cones on acute mouse retinal slices, the presence of GABA-evoked currents with a $GABA_A$ pharmacology. Cone identification was obtained through the inclusion of a morphological dye into the patch pipette, allowing the visualization of the large cone synaptic terminal. Moreover, cones with terminals displayed currents comparable to the calcium-activated chloride currents / glutamate transporter currents detected in

cones from other species (Barnes & Hille, 1989; Verweij *et al.*, 2003; Szmajda & DeVries, 2011). As no synaptic transmission blocker was present in our recording conditions, the GABA-evoked current could correspond to a secondary current following a GABA action on horizontal cell, as observed in the rat retina (Liu *et al.*, 2013) rather than a direct effect on $GABA_A$ receptors present on cone pedicles. It is however unlikely: the recorded current was reversing close to E_{Cl} with a voltage-dependence not compatible with a modulation of the activation curve of cone calcium channels. If that was the case, the maximum effect would have occurred in the -35 to -45 mV range, and minimal effect at potentials bellow -60 mV or over 0 mV. However, the maximal (absolute) amplitude of the GABA-evoked currents was systematically recorded at the most negative potential tested, which was between -102 and -64 mV depending on the recording conditions (Fig. 3 D-F). In addition, outward currents could be recorded above 0 mV for many cones. The most likely explanation is thus that functional $GABA_A$ (and not $GABA_C$) receptors are expressed on mouse cone pedicles. While such a conclusion would have been expected some decades ago when lateral inhibition was considered to result from a GABAergic inhibition of cones, it is now dissonant with a number of published studies, either on the presence of functional GABA receptors on mammalian cone pedicles or on the indirect response of cones to GABA, mediated by horizontal cells.

The apparent discrepancy between our results and the reported presence of both $GABA_A$ and $GABA_C$ currents in cultured pig cones (Picaud *et al.*, 1998) and in mouse cones from flatmount *rd1* retinas or freshly dissociated from C57BL/6J retinas (Pattnaik *et al.*, 2000) can be tentatively explained. In the former case, it could come either from a difference between mouse and pig cones, or a partial dedifferentiation of pig cones after 2 to 10 days in culture. In flatmount *rd1* retinas, cone identity was deduced from the localization in the thin remaining outer nuclear layer at an age at which most rods have degenerated. The recording of both $GABA_A$ and $GABA_C$ currents, larger than the $GABA_A$-only current reported here, could thus be due to a partial dedifferentiation of cones, or to morphological rearrangements occurring during degeneration, with the presence of bipolar cells at the distal surface of the degenerated *rd1* retinas. The former hypothesis is supported by

transcriptome studies from *rd1* cones at more advanced ages (110-220 days), suggesting that the $GABA_C$ ρ_1 and ρ_2 subunit mRNAs are expressed by surviving cones (Busskamp *et al.*, 2010) (see also GEO Series GSE22338). The latter is consistent with the current-voltage relationships of the recorded cells, reminiscent of those of rod bipolar cells. The four freshly dissociated cells from C57BL/6J retinas considered as cones in the same report, may similarly have been bipolar cells with partially damaged/collapsed processes, morphologically close to cones once their pedicle and inner/ outer segments have collapsed, which occurs quickly after dissociation – their current-voltage relationships are also matching those from rod bipolar cells, both in kinetics and in amplitude.

Besides these initial reports, more recent studies suggest that mammalian cones do not express GABA receptors. The lack of a systematic GABA response of macaque cones on flatmount retinas (Verweij *et al.*, 2003), seconded by similar results from David Schneeweis obtained on macaque retinal slices (personnal communication reported in Verweij *et al.*, 2003), indicate that macaque cones do not consistently respond, directly or indirectly, to GABA applications. Similarly, GABA-evoked current were not detected in ground squirrel cones, over a large range of potentials (-110 to +40 mV, Sercan Deniz and Steven DeVries, personal communication). In rat (Liu *et al.*, 2013) and mouse (Kemmler *et al.*, 2014) retinal slices, the effect of GABA on cone calcium signals is not direct but occurs through horizontal cells. In the macaque retina, as surround antagonism was observed in only 20% of the cones (Verweij *et al.*, 2003), the lack of an indirect action of GABA on cones in macaque (and ground squirrel) could be due to the lability of the secondary mechanism relaying horizontal cell membrane potential changes to cones in these species. This mechanism could be more robust in rodent retinas, allowing for a more reliable detection of responses in rat and mouse cones – however not in our case. Both Liu et al. (2013) and Kemmler et al. (2014) prepared slices using a tissue chopper, while we used agarose embedding and vibratome sectioning. Even if it is slower and possibly more mechanically demanding on the tissue due to the blade vibrations, it shouldn't weaken the horizontal cell to cone contact sufficiently to prevent feedback. Studies that did not detect an indirect GABA effect on mammalian cones (Verweij *et al.*, 2003, David Schneeweiss,

Steven DeVries, ours) used patch-clamp recordings of cone currents, while those which did (Liu *et al.*, 2013; Kemmler *et al.*, 2014) relied on calcium imaging. The indirect effect is expected to be mediated by pH changes in the synaptic cleft (Liu *et al.*, 2013), as well as by hemichannels (Kemmler *et al.*, 2014), both resulting in a modulation of the calcium channel activation curve. Whole-cell recordings of cones may perturb this indirect effect, due to the run-down of calcium channel currents. However, we recorded some cones using amphotericin (crossed symbols in Fig. 3E) or gramicidin-perforated patch (Fig. 3F), which should better preserve calcium channel activity over the time course of the experiments. Those cones responded to GABA similarly to those recorded in whole-cell configuration, with no sign of a non-linearity in the potential range affecting calcium channel activation. Another difference between our conditions and those of Liu et al. (2013) and Kemmler et al. (2014) is that we used fully light-adapted retinas. This could tentatively explain the discrepancy between their results and ours, as lateral inhibition is affected by the ambient light level and the light-adaptation state of the retina (reviewed in Thoreson & Mangel, 2012). In Kemmler et al. (2014), the conclusion that "GABA is unlikely acting directly at the [mouse] cone terminal, but instead may modulate cone output by controlling other feedback mechanisms", was based 1) on the fact that the observed changes in calcium signal evoked by GABA puffs in cone pedicles were in contrast to what is expected from a GABAergic inhibition, and 2) on the lack of immunostaining for α_1 and ρ_1 subunits. Neither of these arguments can rule out the presence of $GABA_A$ receptors on cone pedicles: 1) the direct action of GABA on cones depends on E_{Cl}, which most reports point as close to the dark potential: -34 mV in the salamander (Thoreson & Bryson, 2004), -31 mV in the ground squirrel (Szmajda & DeVries, 2011), -37 mV in the putative mouse cones we recorded in the gramicidin perforated-patch configuration. Only a small change in membrane potential is thus expected from the activation of GABA receptors. Moreover, this effect could be masked by the indirect effect mediated by horizontal cells. 2) the presence of the α_1 subunit is not required to have functional $GABA_A$ receptors(reviewed in Olsen & Sieghart, 2008).

The group of Stuart Mangel reported in the recent years an increase in the expression of GABA receptor subunits in rabbit cones during the night (Mangel S, et al. IOVS 2013;54:ARVO E-Abstract 404, Mangel S, et al. IOVS 2015;56:ARVO E-Abstract 1340, Mangel S, IOVS 2016;57:ARVO E-Abstract 588). There was however no recording from rabbit cones to demonstrate that this increase is associated with the presence of functional receptors on the cone terminals. While rabbits are endogenously nocturnal animals, they become predominantly diurnal in animal-house conditions (Jilge, 1991). Thus, similar circadian changes in receptor expression may explain the absence of GABA-evoked current in macaque and ground squirrel cones during the day. Nocturnal animals as rats and mice could be expected to have opposed variations, with $GABA_A$ receptor expression during the day. Our GABA responses recordings from mouse cones were obtained during the day (12 PM – 8 PM), with no evidence of a circadian influence on the current amplitude (Supplementary Figure 4). This time period may have been too short to detect it, but it should also be kept in mind that both mouse lines used in this study are melatonin-deficient (Ebihara *et al.*, 1986), which may prevent circadian changes in receptor expression.

Since the initial demonstration of horizontal cell to cone negative feedback in the vertebrate retina (Baylor *et al.*, 1971), identifying the underlying mechanism(s) has been an active field of research. There is now growing evidence that lateral inhibition results from the compound action of various pathways modulating the pH in the synaptic cleft (Vroman *et al.*, 2014; Warren *et al.*, 2016*a*), including horizontal cell GABA receptors (Liu *et al.*, 2013), together with an ephaptic mechanism (Kamermans *et al.*, 2001; Kamermans & Fahrenfort, 2004; Warren *et al.*, 2016*b*; reviewed in Thoreson & Mangel, 2012; Chapot *et al.*, 2017). The causes of many apparent discrepancies have been progressively identified, but many others still have to be understood. Regarding the influence of GABA on cone responses to center-surround illumination, a confounding factor may have been the low capacity of horizontal cells to counteract the GABA loss happening during retinal harvesting for electrophysiology, as described in the mouse retina (Deniz *et al.*, 2011). This may apply to other species, including those with both a well-established GABAergic nature of horizontal cells and

expression of GABA receptors on cone terminals, as the turtle. If a GABA-dependent feedback was detected only in presence of pentobarbital in slices (Tatsukawa *et al.*, 2005), it may be occurring more robustly *in vivo*. Besides discrepancies, it is unclear why a diversity of modulatory mechanisms coexist in the horizontal cell to cone synapse, or in other words what is the exact contribution of each mechanism depending on the type of stimuli. It is notably hard to predict the role of cone GABA receptors. As mentioned above, many reports indicate that the cone E_{Cl} is close to the dark potential: opening or closing of GABA receptors in response to changes in the GABA release from horizontal cells should then have little direct effect on the cone membrane potential. This effect will be more substantial when the cone E_{Cl} is more negative than the dark potential, as in the turtle or the goldfish (Kaneko & Tachibana, 1986; Kraaij *et al.*, 2000). As cones are graded-potential neurons, even small changes in membrane potential can change the glutamate release. GABA receptors could also contribute through their influence on the synaptic cleft pH, as proposed for those of horizontal cells (Liu *et al.*, 2013), through their permeability to HCO_3^-. Changes in intracellular Cl^- may also affect release, either through the modulation of calcium channels (Thoreson *et al.*, 2000; Babai *et al.*, 2010) or through changes in osmotic tension (Chavas *et al.*, 2004).

Acknowledgements: This work was supported by Human Frontier Science Program grant RGY0004/2003 to MJR, Fédération des Aveugles de France to SD, Association Française contre les Myopathies SAFM05-002 to EW, ANR GABARET to SP, and ANR-10-LABX-0030-INRT, a grant from a French State fund managed by the Agence Nationale de la Recherche under the frame program Investissements d'Avenir ANR-10-IDEX-0002-02, CNRS, INSERM, Université Pierre and Marie Curie, Assistance Publique-Hôpitaux de Paris. We thank Dr. Steve DeVries for his comments on the initial version of this manuscript.

Abbreviations:

BBC: bicarbonate-buffered saline

DIC: Differential Interference Contrast

GABA: γ-amino butyric acid

GCL: ganglion cell layer

HC: horizontal cell

INL: inner nuclear layer

ONL: outer nuclear layer

OPL: outer plexiform layer

TPMPA: (1,2,5,6-Tetrahydropyridin-4-yl)methylphosphinic acid

REFERENCES

Agardh E, Bruun A, Ehinger B & Storm-Mathisen J (1986). GABA immunoreactivity in the retina. *Invest Ophthalmol Vis Sci* **27,** 674–678.

Babai N, Kanevsky N, Dascal N, Rozanski GJ, Singh DP, Fatma N & Thoreson WB (2010). Anion-sensitive regions of L-type CaV1.2 calcium channels expressed in HEK293 cells. *PLoS ONE* **5,** e8602.

Barnes S & Bui Q (1991). Modulation of calcium-activated chloride current via pH-induced changes of calcium channel properties in cone photoreceptors. *J Neurosci* **11,** 4015–4023.

Barnes S & Hille B (1989). Ionic channels of the inner segment of tiger salamander cone photoreceptors. *J Gen Physiol* **94,** 719–743.

Baylor DA, Fuortes MG & O'Bryan PM (1971). Receptive fields of cones in the retina of the turtle. *J Physiol (Lond)* **214,** 265–294.

Brecha NC, Sternini C & Humphrey MF (1991). Cellular distribution of L-glutamate decarboxylase (GAD) and gamma-aminobutyric acid A ($GABA_A$) receptor mRNAs in the retina. *Cell Mol Neurobiol* **11,** 497–509.

Busskamp V, Duebel J, Balya D, Fradot M, Viney TJ, Siegert S, Groner AC, Cabuy E, Forster V, Seeliger M, Biel M, Humphries P, Paques M, Mohand-Said S, Trono D, Deisseroth K, Sahel JA, Picaud S & Roska B (2010). Genetic reactivation of cone photoreceptors restores visual responses in retinitis pigmentosa. *Science* **329,** 413–417.

Cangiano L, Asteriti S, Cervetto L & Gargini C (2012). The photovoltage of rods and cones in the dark-adapted mouse retina. *J Physiol (Lond)* **590,** 3841–3855.

Chapot CA, Euler T & Schubert T (2017). How do horizontal cells 'talk' to cone photoreceptors? Different levels of complexity at the cone–horizontal cell synapse. *J Physiol (Lond)* **595,** 5495–5506.

Chavas J, Forero ME, Collin T, Llano I & Marty A (2004). Osmotic Tension as a Possible Link between $GABA_A$ Receptor Activation and Intracellular Calcium Elevation. *Neuron* **44,** 701–713.

Cueva JG, Haverkamp S, Reimer RJ, Edwards R, Wässle H & Brecha NC (2002). Vesicular gamma-aminobutyric acid transporter expression in amacrine and horizontal cells. *J Comp Neurol* **445,** 227–237.

Davenport CM, Detwiler PB & Dacey DM (2008). Effects of pH buffering on horizontal and ganglion cell light responses in primate retina: evidence for the proton hypothesis of surround formation. *J Neurosci* **28,** 456–464.

Deniz S, Wersinger E, Schwab Y, Mura C, Erdelyi F, Szabó G, Rendon A, Sahel J-A, Picaud S & Roux MJ (2011). Mammalian retinal horizontal cells are unconventional GABAergic neurons. *J Neurochem* **116,** 350–362.

Ebihara S, Marks T, Hudson DJ & Menaker M (1986). Genetic control of melatonin synthesis in the pineal gland of the mouse. *Science* **231,** 491–493.

Fahrenfort I, Steijaert M, Sjoerdsma T, Vickers E, Ripps H, van Asselt J, Endeman D, Klooster J, Numan R, ten Eikelder H, von Gersdorff H & Kamermans M (2009). Hemichannel-mediated and pH-based feedback from horizontal cells to cones in the vertebrate retina. *PLoS ONE* **4,** e6090.

Fletcher EL & Kalloniatis M (1997). Localisation of amino acid neurotransmitters during postnatal development of the rat retina. *J Comp Neurol* **380,** 449–471.

Greferath U, Grünert U, Fritschy JM, Stephenson A, Möhler H & Wässle H (1995). $GABA_A$ receptor subunits have differential distributions in the rat retina: in situ hybridization and immunohistochemistry. *J Comp Neurol* **353,** 553–571.

Greferath U, Grünert U, Müller F & Wässle H (1994). Localization of $GABA_A$ receptors in the rabbit retina. *Cell Tissue Res* **276,** 295–307.

Greferath U, Müller F, Wässle H, Shivers B & Seeburg P (1993). Localization of $GABA_A$ receptors in the rat retina. *Vis Neurosci* **10,** 551–561.

Grigorenko EV & Yeh HH (1994). Expression profiling of $GABA_A$ receptor beta-subunits in the rat retina. *Vis Neurosci* **11,** 379–387.

Guo C, Hirano AA, Stella SL Jr, Bitzer M & Brecha NC (2010). Guinea pig horizontal cells express GABA, the GABA-synthesizing enzyme GAD 65, and the GABA vesicular transporter. *J Comp Neurol* **518,** 1647–1669.

Haverkamp S, Grünert U & Wässle H (2000). The cone pedicle, a complex synapse in the retina. *Neuron* **27,** 85–95.

Hirano AA, Brandstätter JH & Brecha NC (2005). Cellular distribution and subcellular localization of molecular components of vesicular transmitter release in horizontal cells of rabbit retina. *J Comp Neurol* **488,** 70–81.

Hirano AA, Liu X, Boulter J, Grove J, Pérez de Sevilla Müller L, Barnes S & Brecha NC (2016). Targeted Deletion of Vesicular GABA Transporter from Retinal Horizontal Cells Eliminates Feedback Modulation of Photoreceptor Calcium Channels. *eNeuro*; DOI: 10.1523/ENEURO.0148-15.2016.

Hirasawa H & Kaneko A (2003). pH changes in the invaginating synaptic cleft mediate feedback from horizontal cells to cone photoreceptors by modulating Ca^{2+} channels. *J Gen Physiol* **122,** 657–671.

Jackman SL, Babai N, Chambers JJ, Thoreson WB & Kramer RH (2011). A positive feedback synapse from retinal horizontal cells to cone photoreceptors. *PLoS Biol* **9,** e1001057.

Jellali A, Stussi-Garaud C, Gasnier B, Rendon A, Sahel J-A, Dreyfus H & Picaud S (2002). Cellular localization of the vesicular inhibitory amino acid transporter in the mouse and human retina. *J Comp Neurol* **449,** 76–87.

Jeon C-J, Strettoi E & Masland RH (1998). The Major Cell Populations of the Mouse Retina. *J Neurosci* **18,** 8936–8946.

Jilge B (1991). The rabbit: a diurnal or a nocturnal animal? *J Exp Anim Sci* **34,** 170–183.

Kamermans M & Fahrenfort I (2004). Ephaptic interactions within a chemical synapse: hemichannel-mediated ephaptic inhibition in the retina. *Curr Opin Neurobiol* **14,** 531–541.

Kamermans M, Fahrenfort I, Schultz K, Janssen-Bienhold U, Sjoerdsma T & Weiler R (2001). Hemichannel-mediated inhibition in the outer retina. *Science* **292,** 1178–1180.

Kaneko A & Tachibana M (1986). Effects of gamma-aminobutyric acid on isolated cone photoreceptors of the turtle retina. *J Physiol (Lond)* **373,** 443–461.

Kemmler R, Schultz K, Dedek K, Euler T & Schubert T (2014). Differential regulation of cone calcium signals by different horizontal cell feedback mechanisms in the mouse retina. *J Neurosci* **34,** 11826–11843.

Klaassen LJ, Sun Z, Steijaert MN, Bolte P, Fahrenfort I, Sjoerdsma T, Klooster J, Claassen Y, Shields CR, Ten Eikelder HMM, Janssen-Bienhold U, Zoidl G, McMahon DG & Kamermans M (2011). Synaptic transmission from horizontal cells to cones is impaired by loss of connexin hemichannels. *PLoS Biol* **9,** e1001107.

Kraaij DA, Spekreijse H & Kamermans M (2000). The Nature of Surround-Induced Depolarizing Responses in Goldfish Cones. *J Gen Physiol* **115,** 3–16.

Lee H & Brecha NC (2010). Immunocytochemical evidence for SNARE protein-dependent transmitter release from guinea pig horizontal cells. *Eur J Neurosci* **31,** 1388–1401.

Liu J, Li G-L & Yang X-L (2006). An ionotropic GABA receptor with novel pharmacology at bullfrog cone photoreceptor terminals. *Neurosignals* **15,** 13–25.

Liu J, Zhao J-W, Du J-L & Yang X-L (2005). Functional GABA(B) receptors are expressed at the cone photoreceptor terminals in bullfrog retina. *Neuroscience* **132,** 103–113.

Liu X, Hirano AA, Sun X, Brecha NC & Barnes S (2013). Calcium channels in rat horizontal cells regulate feedback inhibition of photoreceptors through an unconventional GABA- and pH-sensitive mechanism. *J Physiol (Lond)* **591,** 3309–3324.

Olsen RW & Sieghart W (2008). International Union of Pharmacology. LXX. Subtypes of γ-Aminobutyric Acid A Receptors: Classification on the Basis of Subunit Composition, Pharmacology, and Function. Update. *Pharmacol Rev* **60,** 243–260.

Pattnaik B, Jellali A, Sahel J, Dreyfus H & Picaud S (2000). $GABA_C$ receptors are localized with microtubule-associated protein 1B in mammalian cone photoreceptors. *J Neurosci* **20,** 6789–6796.

Picaud S, Pattnaik B, Hicks D, Forster V, Fontaine V, Sahel J & Dreyfus H (1998). $GABA_A$ and $GABA_C$ receptors in adult porcine cones: evidence from a photoreceptor-glia co-culture model. *J Physiol (Lond)* **513,** 33–42.

Piccolino M (1995). The feedback synapse from horizontal cells to cone photoreceptors in the vertebrate retina. *Prog Retin Eye Res* **14,** 141–196.

Pottek M, Hoppenstedt W, Janssen-Bienhold U, Schultz K, Perlman I & Weiler R (2003). Contribution of connexin26 to electrical feedback inhibition in the turtle retina. *J Comp Neurol* **466,** 468–477.

Schwartz EA (1987). Depolarization without calcium can release gamma-aminobutyric acid from a retinal neuron. *Science* **238,** 350–355.

Szmajda BA & DeVries SH (2011). Glutamate Spillover between Mammalian Cone Photoreceptors. *J Neurosci* **31,** 13431–13441.

Tachibana M & Kaneko A (1984). gamma-Aminobutyric acid acts at axon terminals of turtle photoreceptors: difference in sensitivity among cell types. *Proc Natl Acad Sci USA* **81,** 7961–7964.

Tatsukawa T, Hirasawa H, Kaneko A & Kaneda M (2005). GABA-mediated component in the feedback response of turtle retinal cones. *Vis Neurosci* **22,** 317–324.

Thoreson WB & Bryson EJ (2004). Chloride equilibrium potential in salamander cones. *BMC Neurosci* **5,** 53.

Thoreson WB & Mangel SC (2012). Lateral interactions in the outer retina. *Prog Retin Eye Res* **31,** 407–441.

Thoreson WB, Nitzan R & Miller RF (2000). Chloride efflux inhibits single calcium channel open probability in vertebrate photoreceptors: chloride imaging and cell-attached patch-clamp recordings. *Vis Neurosci* **17,** 197–206.

Vardi N, Masarachia P & Sterling P (1992). Immunoreactivity to $GABA_A$ receptor in the outer plexiform layer of the cat retina. *J Comp Neurol* **320,** 394–397.

Vardi N & Sterling P (1994). Subcellular localization of $GABA_A$ receptor on bipolar cells in macaque and human retina. *Vision Res* **34,** 1235–1246.

Versaux-Botteri C, Pochet R & Nguyen-Legros J (1989). Immunohistochemical localization of GABA-containing neurons during postnatal development of the rat retina. *Invest Ophthalmol Vis Sci* **30,** 652–659.

Verweij J, Hornstein EP & Schnapf JL (2003). Surround antagonism in macaque cone photoreceptors. *J Neurosci* **23,** 10249–10257.

Verweij J, Kamermans M & Spekreijse H (1996). Horizontal cells feed back to cones by shifting the cone calcium-current activation range. *Vision Res* **36,** 3943–3953.

Vroman R, Klaassen LJ, Howlett MHC, Cenedese V, Klooster J, Sjoerdsma T & Kamermans M (2014). Extracellular ATP Hydrolysis Inhibits Synaptic Transmission by Increasing pH Buffering in the Synaptic Cleft. *PLoS Biol* **12,** e1001864.

Wang T-M, Holzhausen LC & Kramer RH (2014). Imaging an optogenetic pH sensor reveals that protons mediate lateral inhibition in the retina. *Nat Neurosci* **17,** 262–268.

Warren TJ, Hook MJ, Supuran CT & Thoreson WB (2016*a*). Sources of protons and a role for bicarbonate in inhibitory feedback from horizontal cells to cones in Ambystoma tigrinum retina. *J Physiol (Lond)* **594,** 6661–6677.

Warren TJ, Hook MJV, Tranchina D & Thoreson WB (2016*b*). Kinetics of Inhibitory Feedback from Horizontal Cells to Photoreceptors: Implications for an Ephaptic Mechanism. *J Neurosci* **36,** 10075–10088.

Wu SM (1986). Effects of gamma-aminobutyric acid on cones and bipolar cells of the tiger salamander retina. *Brain Res* **365,** 70–77.

Wu SM (1992). Feedback connections and operation of the outer plexiform layer of the retina. *Curr Opin Neurobiol* **2,** 462–468.

FIGURE LEGENDS

Figure 1: **Distinguishing cones from rods through their morphology**. (A-B) Superposition of DIC images from retinal slices and fluorescence images, and fluorescence images only, of recorded cones, filled with Alexa Fluor 488. Cones had an oval soma (s) and a large terminal (t). Stars (*) indicate putative cone somas. (C) Confocal image from a cone filled with Alexa Fluor 488 acquired after recording. (D-E) Superposition of DIC images from retinal slices and fluorescence images, and fluorescence images only, of recorded rods, filled with either Alexa Fluor 488 or 594. The smaller rounded somas and terminals contrast with those of cones. Scale bars: 10 µm in C, 20 µm in other panels.

Figure 2: **Electrophysiological signature of cones and rods**. (A-B) Representative currents evoked by voltage-jumps in a cone (A) and in a rod (B), from a holding potential of -74 mV, with 100 ms steps to potentials ranging from +46 mV to -134 mV by 20 mV decrements (E_{Cl} = -29 mV intra-pipette solution). The magenta horizontal bar indicates the period considered to measure the "plateau" current, as plotted in D, F and G; the green arrow indicates the time at which the tail current was measured, 13 ms after repolarization, as plotted in panels E, F and G. (C) Currents evoked by voltage-jumps in a cone as in A, with a longer time scale to show the full deactivation of the Ca^{2+}-dependent Cl^- current. The interval between steps was 10 s to allow for a full deactivation of this current. (D) Current-voltage relationship of the current evoked by 100 ms voltage jumps, from a holding potential of -74 mV, to potentials ranging from +46 mV to -134 mV by 10 mV decrements (E_{Cl} = -29 mV intra-pipette solution), measured from 97 to 99 ms following depolarization, for morphologically identified rods (black circles, n = 13) and cones (open circles, n = 11). (E) Current-voltage relationship of the tail current measured 13 ms after returning to the holding potential of -74 mV, following 100 ms voltage jumps to potentials ranging from +46 mV to -134 mV by 10 mV decrements (E_{Cl} = -29 mV intra-pipette solution), for rods (black circles, n = 13) and cones (open circles, n = 11). (F-G) Individual

values of the "plateau" current measured at +26 mV (F) or the tail-current measured after a depolarization at +6 mV (G) for rods (grey symbols when spherule is present, n = 13; orange symbols for rods for which no spherule could be seen at the end of the recording but identified as rods through their external segment, n = 11), putative rods (cyan symbols, for cells considered as putative rods due to their soma appearance prior to patching, n = 5), cones (green symbols, presence of a pedicle, n = 11) or putative cones (red symbols, cells for which no pedicle could be seen at the end of the recording, but with a soma appearance suggestive of a cone prior to recording, n = 8). Triangles are used for rods in which an intact outer segment could be identified at the end of the recording, circles are used for other cells. The dotted line delimits the [I_{tail} < 100 pA, $I_{plateau}$ < 350 pA] range, which includes all identified and putative rods, and only one of the identified or putative cones.

Figure 3: Cone responses to GABA have a $GABA_A$ pharmacology. (A) Puff application of GABA (100 ms, 1 mM) in the vicinity of a photoreceptor terminal evoked a current in cones (left) but not in rods (right). The holding potential was -74 mV, as in B and C. (B) Cone responses to puff application of GABA (100 ms, 1 mM, control trace in black) were blocked by 100 µM bicuculline methiodide (left, red trace) but not by 50 µM TPMPA (right, blue trace). Traces obtained following wash out of the applied drug are shown in grey. (C) As in B, but for a cone which GABA response was not fully blocked by 100 µM bicuculline methiodide (left, red trace). The right panel represents the traces from the left panel normalized to their peak, showing that the remaining component has the same kinetics as the control and wash currents. (D-E) Currents evoked by GABA reversed close to E_{Cl}, whether it was set close to -29 mV (D, 5 cells) or 2 mV (E, 6 cells), depending on the intrapipette solution. The calculated E_{Cl} is represented by a red line for reference. Each cell is plotted with a given color and distinct symbols linked by a dashed line. (F) GABA-evoked currents as a function of membrane potentials for

4 cones recorded using gramicidin perforated patch. Data points of a given cell are linked by a dashed line; solid lines are linear regressions to the data points.

A
B
C
os
is
s
t
a
D
E

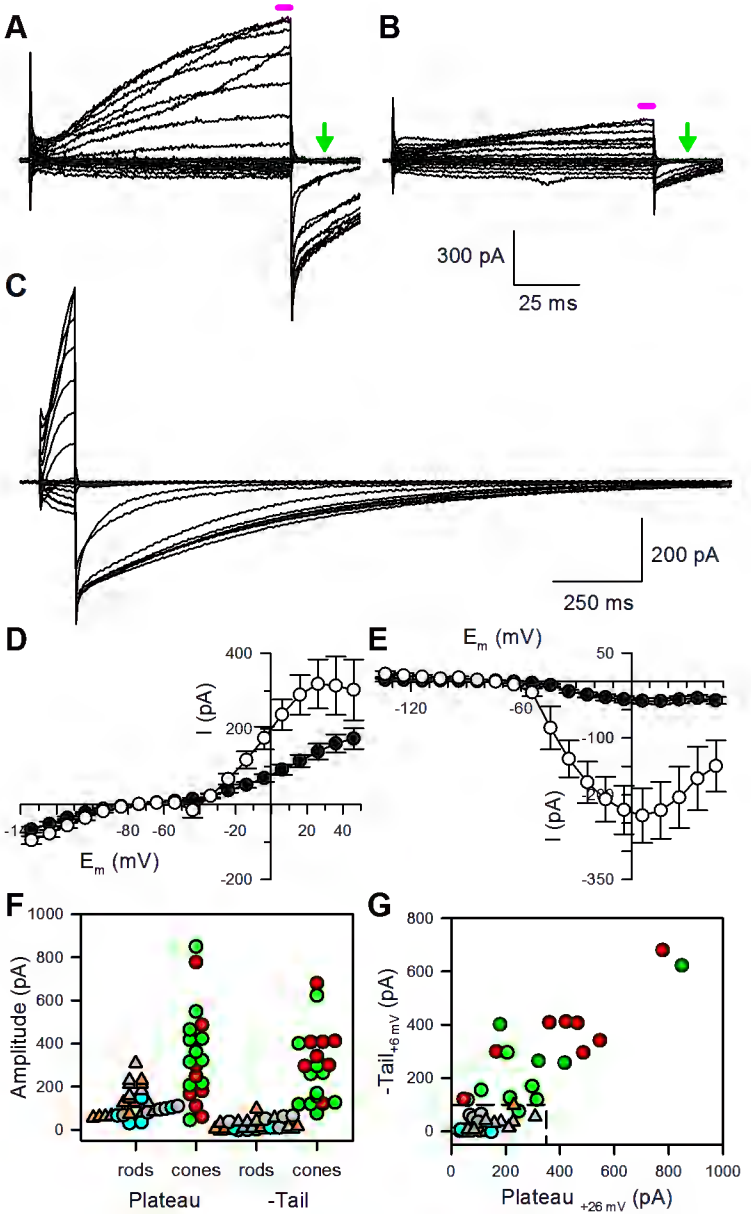
A
B
300 pA
25 ms
C
200 pA
250 ms
D
I (pA)
400
200
-200
-80
-60
-20
20
40
E_m (mV)
E
E_m (mV)
50
-120
-60
-100
I (pA)
-350
F
Amplitude (pA)
1000
800
600
400
200
0
rods
cones
rods
cones
Plateau
-Tail
G
-Tail_+6 mV (pA)
800
600
400
200
0
0
200
400
600
800
1000
Plateau_+26 mV (pA)

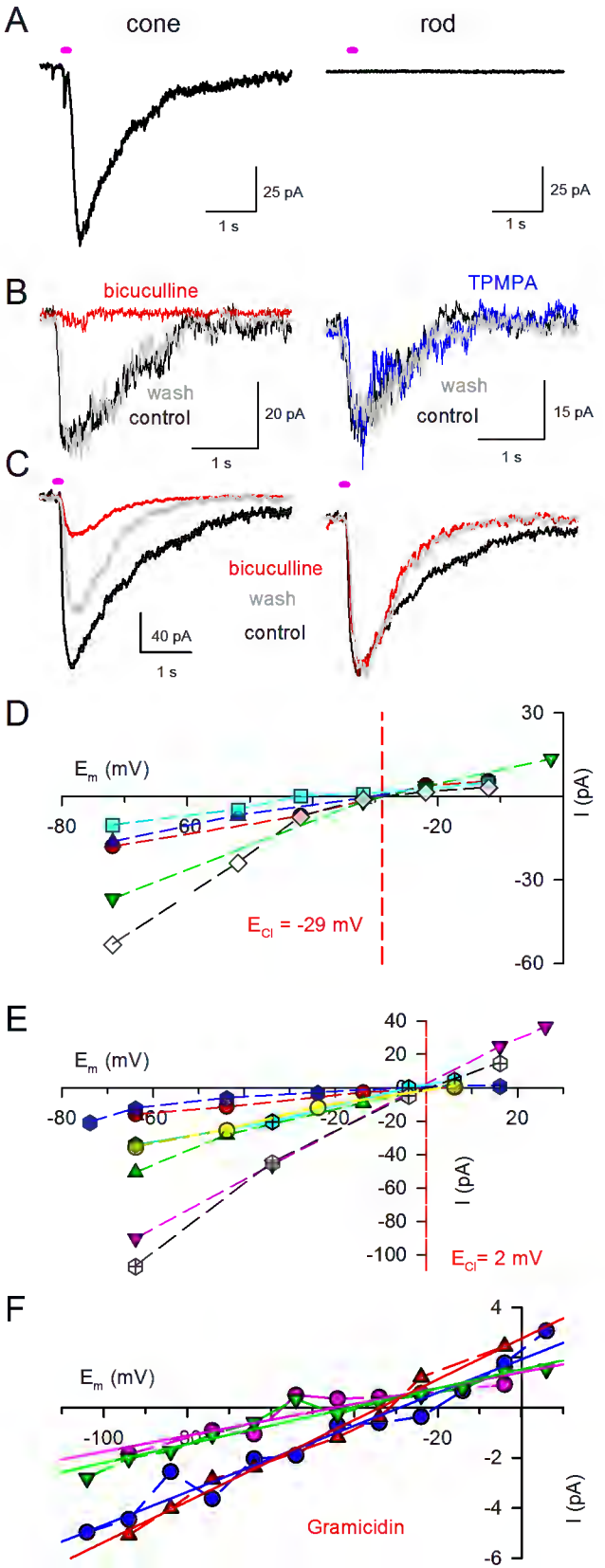
A
cone
rod
25 pA
1 s
25 pA
1 s
B
bicuculline
wash
control
20 pA
1 s
TPMPA
wash
control
15 pA
1 s
C
bicuculline
wash
control
40 pA
1 s
D
E_m (mV)
-80
-60
-20
30
-30
-60
I (pA)
E_Cl = -29 mV
E
E_m (mV)
-80
-60
-20
20
40
20
-20
-40
-60
-80
-100
I (pA)
E_Cl = 2 mV
F
E_m (mV)
-100
-80
-20
4
-2
-4
-6
I (pA)
Gramicidin

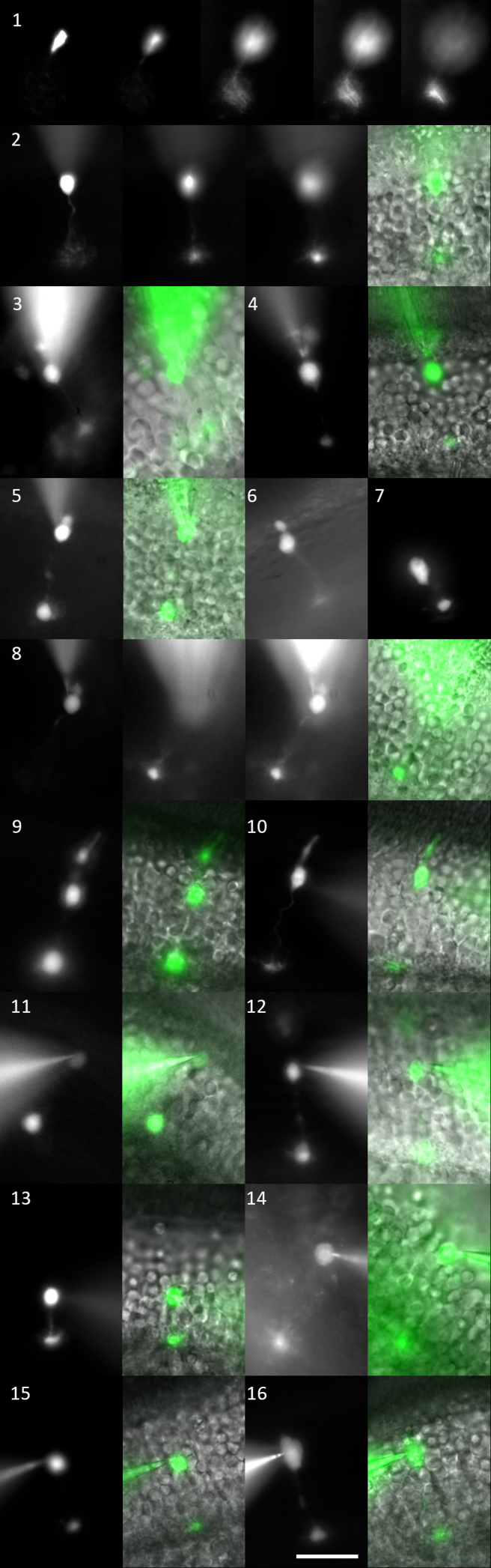
1
2
3
4
5
6
7
8
9
10
11
12
13
14
15
16

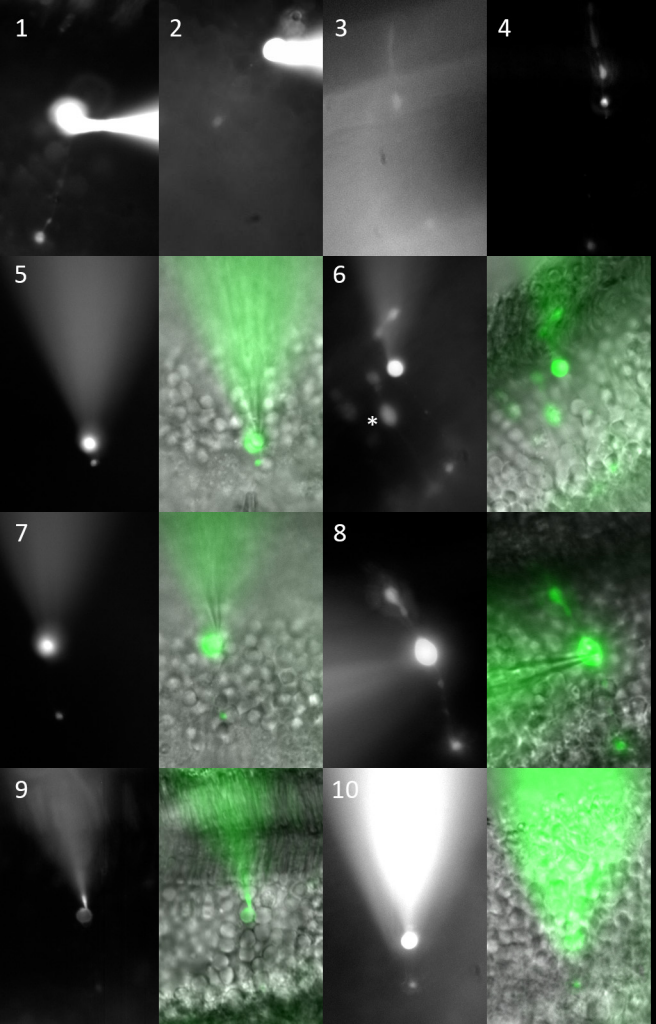
1
2
3
4
5
6
*
7
8
9
10

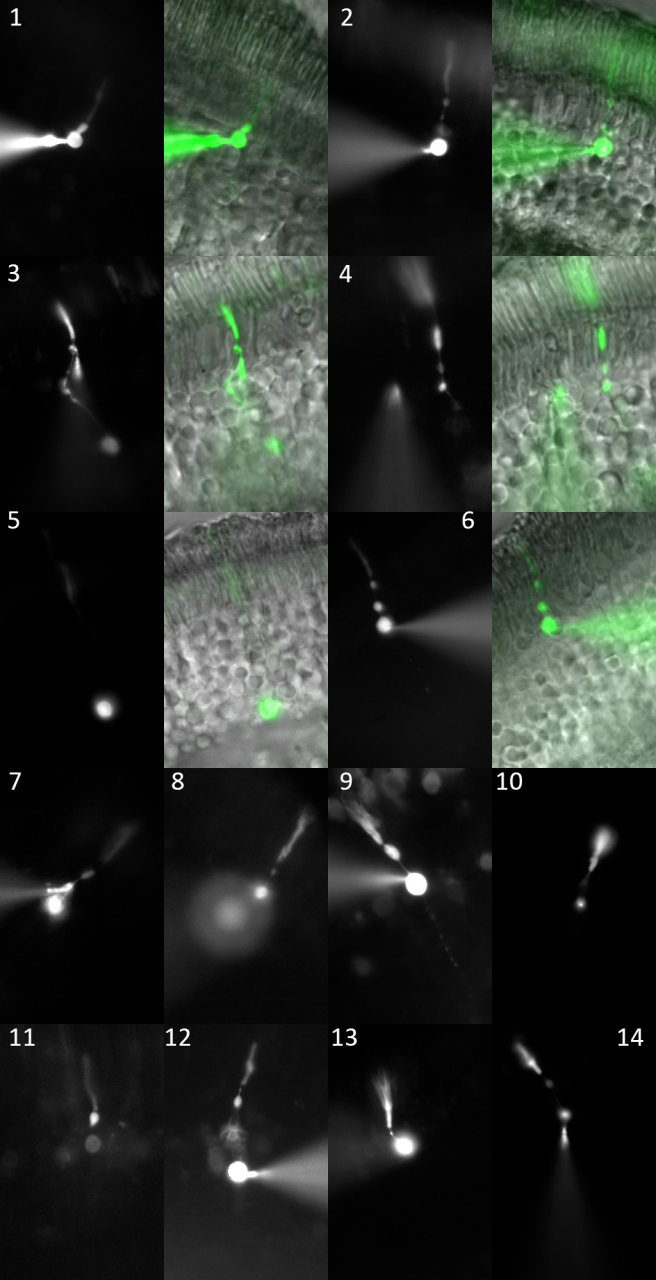
1
2
3
4
5
6
7
8
9
10
11
12
13
14

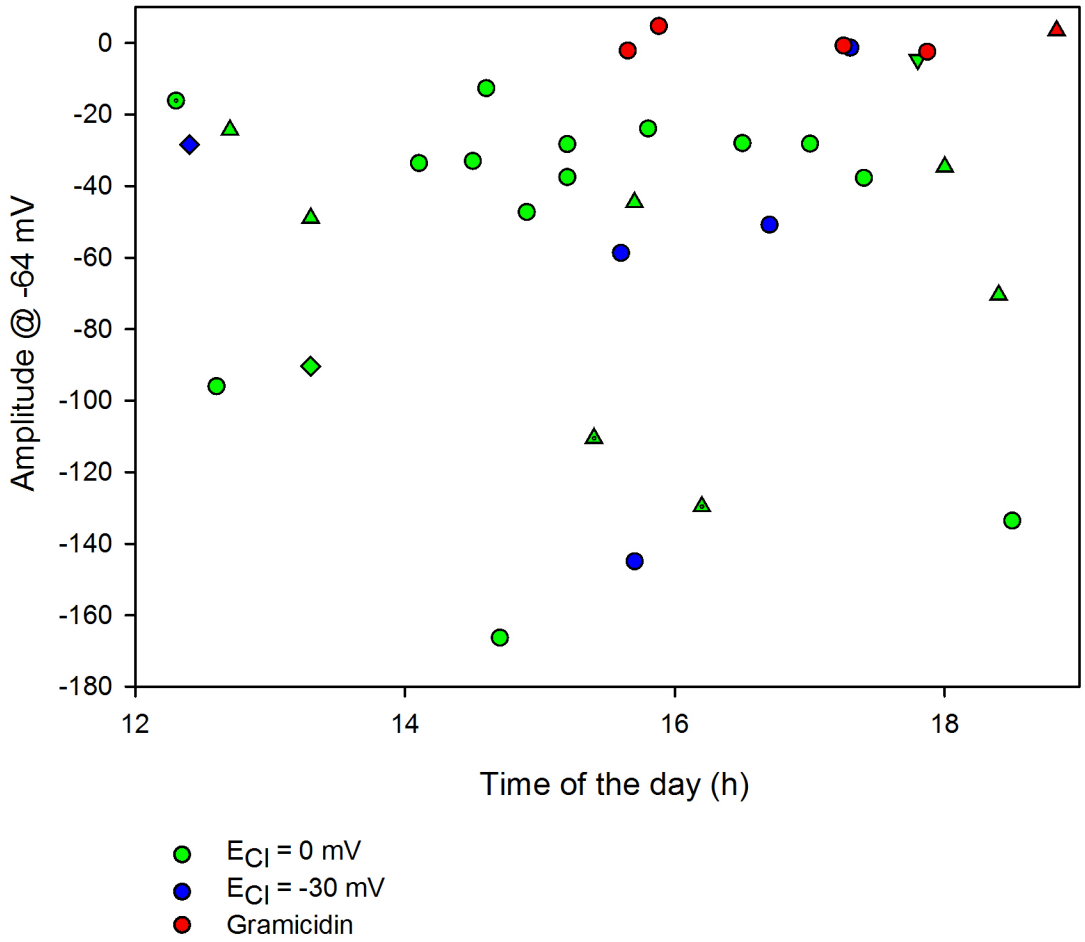
0
-20
-40
-60
-80
-100
-120
-140
-160
-180
Amplitude @ -64 mV
12
14
16
18
Time of the day (h)
E_Cl = 0 mV
E_Cl = -30 mV
Gramicidin

Legends of Supplementary Figures

Supplementary Figure 1: Cones with pedicle

Morphology of 16 recorded cones with their pedicle, obtained through the inclusion of an Alexa dye in the intrapipette solution. For cones 1,2 and 8,, images taken at different depth of focus are represented. For 13 of them, superimposition with a DIC image of the ONL/OPL is also presented. Scale bar in 16: 30 µm.

Supplementary Figure 2: Rods with spherule

Morphology of ten recorded rods with their spherule. For rods 2 and 3, the image was taken after retrieval of the patch pipette, to which the cell soma remained attached. In 6, a cone previously recorded is labeled with a *, next to the brighter rod.

Supplementary Figure 3: Rods with outer segment but without spherule

Morphology of 14 recorded rods identified through the presence of a long, thin outer segment, but which had lost their spherule during the slicing process.

Supplementary Figure 1: Amplitude of the GABA-evoked current as a function of the time of recording.

Amplitude of the current evoked by a 1 mM GABA puff of duration 5-10 (◇), 50 (△), 100 (○) or 250 ms (▽). Recordings were obtained with intrapipette solutions with E_{Cl} = -30 mV (blue symbols) or E_{Cl} = 0 mV (green symbols, open for while-cell, dotted symbols for amphotericin perforated patch). For cones not recorded with the E_{Cl} = 0 mV intracellular solution, the current amplitude was corrected for the difference in driving force. Recordings obtained using gramicidin perforated patch are indicated by red symbols, and were left uncorrected